anpet
brazilian association for transportation research and education
TRANSPORTES
ISSN: 2237-1346
anpet.org.br/transportes

Laboratory and numerical analysis for enhanced ballast performance: towards sustainable railway track pavement design

Uma análise laboratorial e numérica do desempenho de materiais de lastro: em direção à sustentabilidade no projeto de pavimentos ferroviários

André Fardin Rosa[1,2], Stefanie de Carla Dias[2,3], Wescley Silva Brito[2], Robson Correia Costa[1], Edson de Moura[1], Liedi Légi Bariani Bernucci[1], Rosângela dos Santos Motta[1]

[1]Universidade de São Paulo, São Paulo, São Paulo, Brasil
[2]Rumo S.A., Curitiba, Paraná, Brasil
[3]Instituto Militar de Engenharia, Rio de Janeiro, Rio de Janeiro, Brasil

Contact: andrefardinrosa@usp.br, (AFR); stefanie.dias@rumolog.com, (SCD); wescley.brito@rumolog.com (WSB); robsoncosta@usp.br, (RCC); edmoura@usp.br (EM); liedi@usp.br, (LLBB); rosangela.motta@usp.br, (RSM)

Submitted:
7 July, 2024
Revised:
11 November, 2024
Accepted for publication:
14 December, 2024
Published:
14 March, 2025
Associate Editor:
Francisco Thiago Sacramento Aragão, Universidade Federal do Rio de Janeiro, Brasil

Keywords:
Railway.
Track design.
Ballast characterization.
Ballast thickness.
FEM analysis.

Palavras-chave:
Ferrovia.
Dimensionamento.
Caracterização do lastro.
Espessura do lastro.
Elementos finitos.

DOI: 10.58922/transportes.v33.e3028

ABSTRACT
The physical and mechanical characterization of rock materials is a crucial step for their applicability as a railway ballast layer. However, most of the standardized tests for such characterization do not have direct application for the ballast layer design and the normative limits take into account only the origin of the rock material, ignoring the axle load factor and the lifespan for which the railway project is designed. This study aims to demonstrate the importance of characterizing materials in this process, through laboratory tests (physical and mechanical) and finite element modeling with four different rock materials as ballast, applying the results to obtain a reduction in the use of stone materials, aiming an optimized and sustainable concept for new railway projects. The effects of ballast thickness on subgrade stresses are analyzed in terms of subgrade bearing capacity and permanent deformation of geotechnical materials. The results show that variations in the ballast's resilience modulus between 294 and 115 MPa have minimal influence on the subgrade's vertical stresses, but that reductions of 10 cm in the thickness of this layer can increase subgrade stresses by up to 20%. Furthermore, an increase in the number of non-cubic particles can lead to greater permanent deformations, which can reduce the period between track maintenance cycles. Finally, the analysis showed that the Micro-Deval test can be considered an interesting method for the mechanical characterization of ballast and can be used to estimate its lifespan.

RESUMO
A caracterização física e mecânica de materiais rochosos é uma etapa determinante para a sua aplicabilidade como camada de lastro ferroviário. Porém, a maioria dos ensaios normatizados para tal caracterização não tem aplicação direta no dimensionamento da espessura da camada de lastro e os limites normativos levam em consideração apenas a origem da rocha, ignorando fatores de carga por eixo e vida útil para a qual a ferrovia é projetada. Este estudo visa demonstrar a importância da caracterização dos materiais neste processo, por meio de ensaios laboratoriais (físicos e mecânicos) e modelagem por elementos finitos com quatro diferentes materiais rochosos como lastro, sendo os resultados aplicados na redução do uso de materiais pétreos em projetos de novas ferrovias brasileiras, para uma construção mais otimizada e sustentável. Os efeitos da espessura do lastro nas tensões do subleito são analisados em termos de capacidade de suporte do subleito e deformação permanente dos materiais geotécnicos. Os resultados mostram que variações de módulo de resiliência no lastro entre 294 e 115 MPa tem influência mínima nas tensões verticais do subleito, mas que reduções de 10 cm na espessura dessa camada podem aumentar em até 20% as tensões no subleito. Além disso, um aumento no número de partículas não cúbicas pode levar a maiores deformações permanentes, o que pode reduzir o período entre ciclos de manutenção da via. Por fim, as análises mostraram que o teste Micro-Deval pode ser considerado como um método interessante para a caracterização mecânica do lastro, podendo ser utilizado para estimar a sua vida útil.

1. INTRODUCTION

Granular materials in ballasted railways provide a stable foundation upon which the rails, fastening system and sleepers will distribute the train loads. In terms of mechanical role, the ballast must be designed with a specific depth, together with the underlayers, to avoid subgrade failure, as well as to reduce track settlement. These characteristics are achieved, among other things, by varying the ballast layer thickness and comparing the stresses acting on the subgrade in conjunction with the bearing capacity (Li et al., 2016).

Another important characteristic of a good ballast material is its durability, which is related to the rock material's ability to withstand weather variations, such as freeze-thaw cycles and wetting-drying, while being subjected to heavy train loads (Watters, Klassen and Clifton, 1987). In this context, the performance and the longevity of the railway infrastructure plays a pivotal role in promoting sustainability for the system.

In the present study, the evaluation of railway ballast goes beyond the standard procedure analysis, considering aspects such as the estimated ballast lifespan, stress attenuation capacity related to subgrade failure and stability against track permanent deformations. A comprehensive characterization of ballast materials is employed and a mechanical analysis using finite elements modeling is performed. These concepts are applied with the aim to reduce the consumption of stone materials and reduce environmental impacts for a new railway project, in a region where qualified ballast material is rarely found, resulting in long transport distances for the material.

Subgrade stresses and bearing capacity

In determining the stresses acting on the subgrade, an important step involves defining the constitutive models for the track components, such as the geotechnical materials. The resilient modulus (R_M) of granular materials is defined as a parameter that is dependent mainly on confining stress, but also on deviatoric stress at some extent (Lackenby et al., 2007; Sun, Indraratna and Nimbalkar, 2016). Therefore, the combined model (Uzan, 1985) was selected to represent the resilient behavior of both the ballast and the subgrade. The model is described in Equation 1, where k_1, k_2, k_3 are the regression coefficients, σ_3, σ_d are the stress components, and p_0 is the reference atmosphere pressure, for unit compatibility.

$$R_M = k_1 \left(\frac{\sigma_3}{p_0} \right)^{k_2} \left(\frac{\sigma_d}{p_0} \right)^{k_3} \tag{1}$$

In the railway track design, each layer's thickness is calculated based on its properties and the mechanical strength of underlying layers. The last step of this calculation procedure consists in verifying if the peak stresses acting at the subgrade are below the subgrade bearing capacity (SBC) (Doyle, 1980). AREMA manual suggests that SBC should not exceed 138 kPa, independently of the subgrade material.

The Broms method (Sattler et al., 1989) was developed for determining the subgrade ultimate stress (q_u) for highways and is considered an adaptation of the Terzaghi method. The analysis considers the impact of soil shear resistance, loading geometry, and surcharge on determining the soil bearing capacity, as presented in Equation 2. The parameters N_c, N_γ, N_q are bearing capacity factors, c is the foundation soil cohesion, γ is the unit weight of overlying layers, B is the width of the footing and q_0 the surcharge loading.

$$q_u = cN_c + 0.5\gamma BN_\gamma + q_0 N_q \quad (2)$$

The key concept of this method is to evaluate the potential shear failure in subgrade material when subjected to distributed loads exceeding the soil's ultimate strength. Shear parameters of subgrade soil can be determined using direct shear or static triaxial tests on undisturbed soil samples, yielding values for the internal friction angle ($\varnothing$), cohesion, and natural unit weight. Since these laboratory tests are conducted under static conditions, a safety factor of 2.5 or 3 is typically applied to derive the safe bearing capacity (SBC) from the ultimate bearing capacity q_u (AREMA, 2020; Sattler et al., 1989).

Geometry degradation

The geotechnical materials plays an important role to prevent track geometry degradation, mainly because even compacted soils tend to accumulate strains in each loading cycle, until these strains are stabilized or the progressive failure occurs (Werkmeister, Dawson and Wellner, 2001).

There are different ways to study the relation between loading cycles and permanent deformation. The most simple consists in adjusting (for each cyclic triaxial test stress state) the mathematical model presented in Equation 3 (Monismith, 1976), where a,b are regression coefficients, N is the number of cycles and ε_p is the accumulated permanent deformation.

$$\varepsilon_p = aN^b \quad (3)$$

Other way is to build a relationship between stress state, number of cycles and permanent deformation, then in this case the cyclic triaxial results can be adjusted to a more generalized model (Guimarães, 2009; Lima and Motta, 2016). The model is presented in Equation 4, with $\psi_1,\psi_2,\psi_3,\psi_4$ as regression coefficients and σ_3,σ_d the stress inputs.

$$\varepsilon_p = \psi_1 \left(\frac{\sigma_3}{p_0}\right)^{\psi_2} \left(\frac{\sigma_d}{p_0}\right)^{\psi_3} N^{\psi_4} \quad (4)$$

Ballast lifespan

One of the main causes of ballast degradation is ballast fragmentation and wear. The resistance to fragmentation may be experimentally evaluated through the Los Angeles Abrasion test, while wear may be assessed through the Micro-Deval or Mill Abrasion tests (Selig and Boucher, 1990). From field observations and laboratory tests, the Canadian Pacific Railroad (CPR) developed a relation between ballast degradation and the abrasion number (AN), which is the sum of the LAA value and five times the mill abrasion result. Although this relationship was developed for a 30 t/axle railway, it could be used as a comparative among different ballast materials under other loading conditions. It is worth mentioning that the original equation uses the Mill Abrasion value, which is interchangeable with the Micro-Deval value, and the result is expressed in "short ton", that can be converted into ton "t", resulting in Equation 5 for concrete sleepers (Ramūnas et al., 2017). In Equation 5, $\frac{L_G}{B}$ is the ballast lifespan for a track with concrete sleepers, measured in transported million gross tons (MGT), LAA and M_{DE} are Los Angeles and Micro-Deval results in %.

$$\frac{L_G}{B} = 1.029\left(10^6 exp\left(8.08 - 0.0382\left(LAA + 5M_{DE}\right)\right)\right) \quad (5)$$

Case study

The Ferronorte extension is a project by Rumo S.A. in Brazil, consisting of approximately 740 km inside the state of Mato Grosso (Figure 1). Located at the north part of the Paraná basin, the railway line will cross predominantly sedimentary rock formations, especially sandstones. Due to this factor, ballast materials composed of igneous or metamorphic rocks are scarce and obtaining appropriated material normally requires long transportation distances. The procedure followed for full ballast evaluation and selection in track design is depicted in Figure 2.

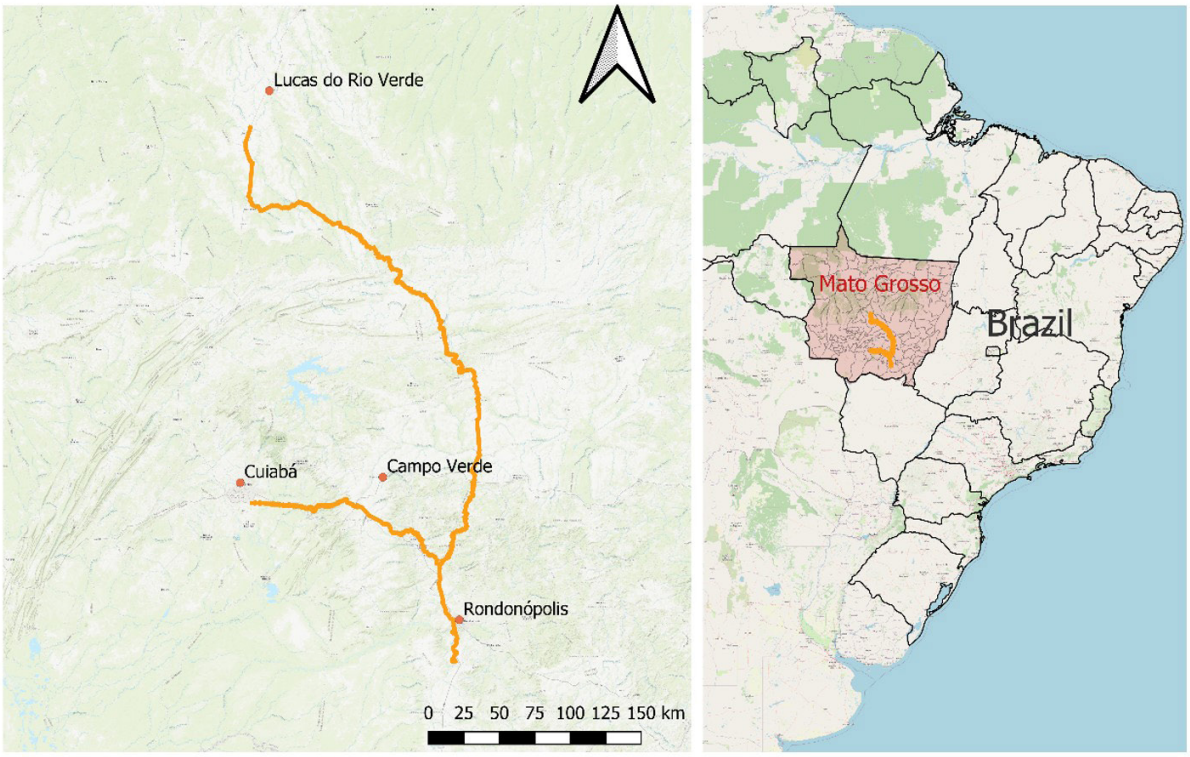

Figure 1. Location of the Railway Construction.

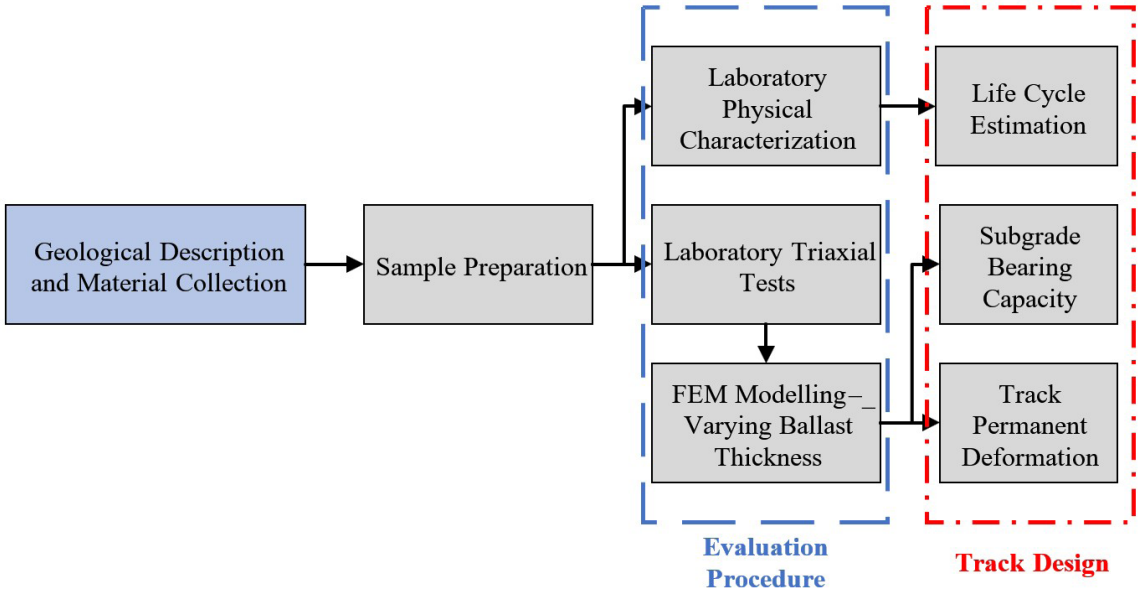

Figure 2. Study Flowchart.

2. PHYSICAL AND PARTICLE STRENGHT EVALUATION

2.1. Geological description

During the prospection for ballast materials, four quarries were identified and studied (Figure 3), named from Q-1 to Q-4. While Q-1 is approximately 50 km from the current terminal where construction begins, the other three quarries are located between 150 and 300 km from the same reference point. This distance increases as construction progresses.

First, a geological characterization was performed with rock massif visual description, thin section petrographic analysis (DNIT 435/2021, similar to ASTM C 295) and X-ray diffractometry, both in qualitative and semiquantitative approaches.

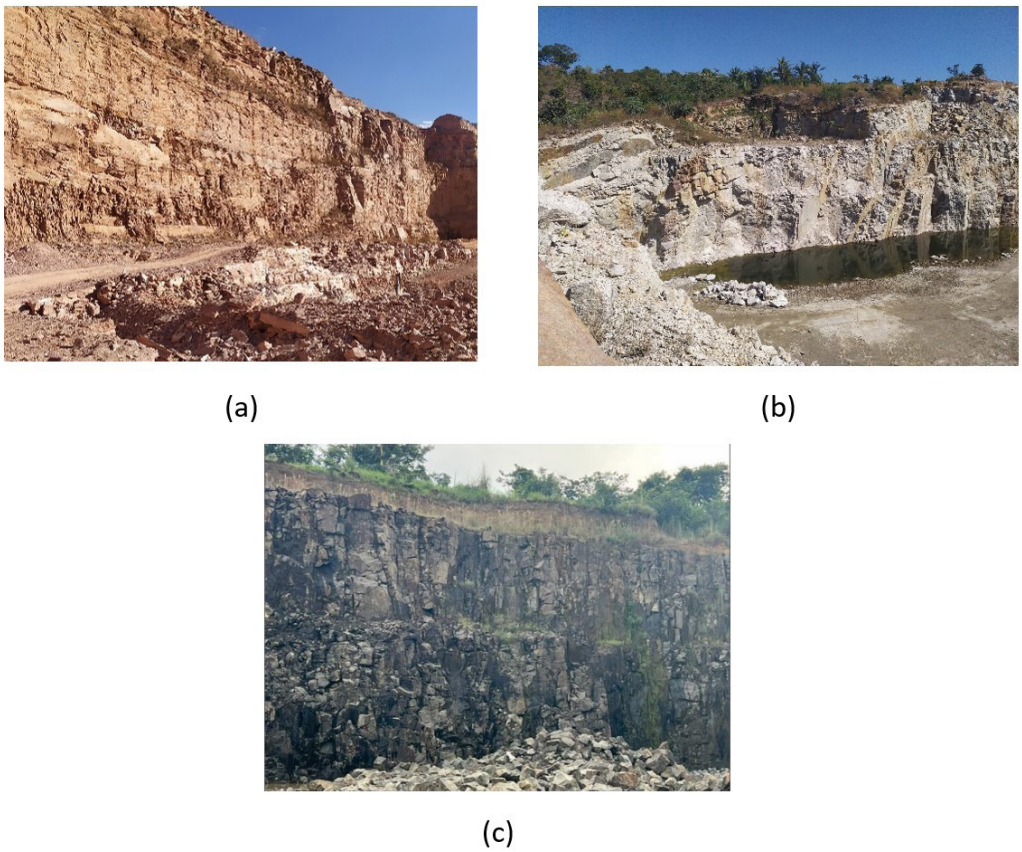

Figure 3. Quarries visual aspect: (a) Q-1; (b) Q-2 and Q-3, (c) Q-4.

Q-1 is located at Furnas Formation and the material is composed of sandstones, varying its weathering degree and joint spacing in depth. The bottom part of the quarry, located about 30 m from the top, is under exploration and shows a less weathered rock, thus it was the portion chosen for the present study. In laboratory, it was identified that Q-1 material is mainly composed of small quartz crystals (81%) and kaolinite (15%). The high hardness of both the quartz crystals and the kaolinite mineral matrix gives the rock a less friable character, despite its sedimentary nature. The texture of the rock is fine and homogeneous, without a clear bedding pattern, which would comprise the particle resistance to loading.

Q-2 and Q-3 materials were extracted from two quarries in the same region at São Vicente formation, and they are characterized as granites. At the quarries, it was identified a very homogeneous and coarse-grained material. Both materials are composed of about 32% quartz,

31% albite, 30% microcline and 5% muscovite. Due to the low presence of biotite, the particles are light in color. The texture is uneven, defined by tabular and elongated crystals of feldspar structures with hydrothermal alteration and rounded recrystallized quartz. Although the materials have shown small content of mica, which is a soft mineral and is proven to negatively correlate with rock resistance (Nålsund, 2014; Rosa, 2019; Trotta, 2020), the feldspar hydrothermal alteration could negatively affect the particles mechanical resistance.

Quarry Q-4 is located inside the Serra Geral formation and the material is characterized as basalt. The mining front in activity is homogeneous, with only some small portions of weathered material. The collected particles have shown a composition of approximately 56% plagioclase, 38% clinopyroxene and 4% volcanic glass and 2% of other opaque minerals. Finally, the material appears to be isotropic and without visual flaws.

2.2. Laboratory characterization

The samples were collected and transported to laboratory for physical and mechanical characterization, following the Brazilian procedure NBR 5564 (ABNT, 2021), which is similar to test standards recommended by AREMA for ballast aggregate. First, the material was quartered to ensure the use of representative samples for the tests, during this process it was observed that material from Q-1 was significantly coarser than the conventional ballast materials, while material from Q-3 was visually finer than expected. Although the latter characteristic would lead to the disapproval of the materials, it reflects the current settings of the quarry production, which could be adjusted in the future to follow the recommendations appropriately. The particle-size distributions (PSDs) are shown in Figure 4, along with the limits of EN-13450 and NBR 5564 (ABNT) standards.

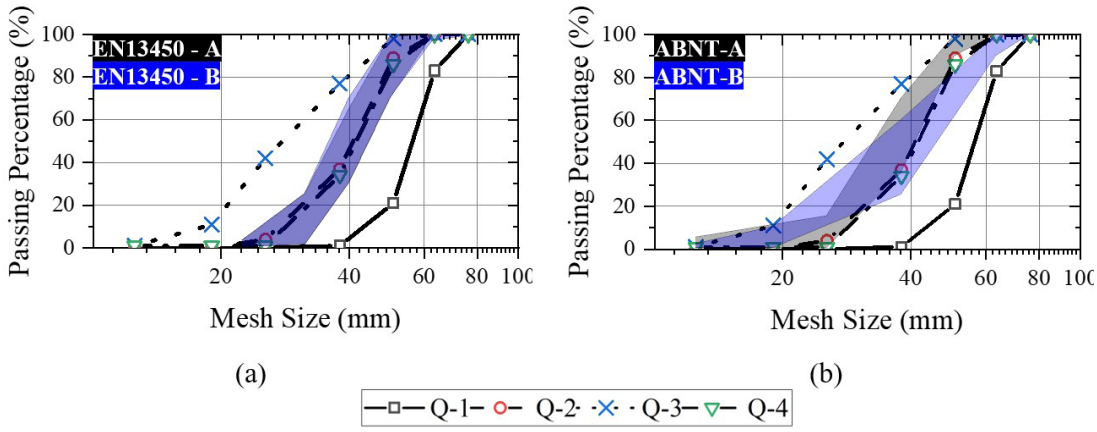

Figure 4. Particle-Size Distribution Limits: (a) AREMA; (b) EN-13450.

The characterization results are summarized in Table 1, along with the standard limits considering each quarry lithology. From the characterization results it was observed that the Q-1 material showed a percentage of clay lumps above 0.5% and elevated porosity, resulting in high values of apparent porosity, absorption, and low apparent density. It was expected that the porosity would significantly affect the mechanical resistance, but the material performed well in both L.A.A. (Los Angeles Abrasion) and Treton Index. The Q-1 material was the only one to fail the UCS (Unconfined Compress Strength) limit of 100 MPa recommended by NBR 5564, with a result of 83 MPa. The materials from Q-2, Q-3, and Q-4 met the majority of the standard parameters, except for the high non-cubic percentage, significantly above the 5% standard limit.

Even though it was identified that the material from Q-1 has high porosity and fails the UCS limits, the mechanical and weathering tests performed in particle samples indicated that the material would not degrade quickly in service. Although the high porosity may be associated with degradation due to the water volume variation in freeze-thaw situations (Watters, Klassen and Clifton, 1987), this is not a concern on most Brazilian railway projects, situated in a tropical region. On the other side, the water effect on ballast degradation is a concern in Brazil, due to the seasons marked with heavy rainfalls and often insufficient drainage devices. For this reason, it was decided to perform the Micro-Deval (M_{DE}) test and investigate whether the ballast mechanical behavior would be affected by the presence of water (Santos et al., 2021).

After 12,000 rotations, the materials were sieved using 1.7 mm sieve and dried, Q-1 exhibited a 26.9% mass loss, Q-2 lost 9.5% of mass, Q-3 lost 14.5% and Q-4 presented 9.7% mass loss. The test conclusively identified significant differences between materials Q-1 and Q-4, indicating that Q-1 is prone to considerable degradation in the presence of water. Additionally, the M_{DE} results for Q-1 and Q-3 material exceeded the limits specified in EN-13450 (14%).

These results underscore the necessity of incorporating a water abrasion test into the Brazilian standards. Despite the latest ballast standard introducing the M_{DE} test, it remains non-mandatory at present.

The ballast degradation due to traffic loads can be estimated using Equation 5, which considers the ballast toughness and abrasion resistance, determined using LAA and M_{DE} respectively. The results are shown in Figure 5.

Table 1: Quarries laboratory characterization limits and results.

Parameter	Units		Q-1	Q-2	Q-3	Q-4
Apparent Density	g/cm^3	Result	2.20	2.62	2.59	2.94
		Limit	>2.50	>2.60	>2.60	>2.70
Apparent Porosity	%	Result	7.62	0.7	1.3	1.52
		Limit	<2	<2	<2	<2
Absorption	%	Result	3.47	0.26	0.5	0.52
		Limit	<2	<1	<1	<1
Non-cubic	%	Result	4	21	31	33
		Limit	<15	<15	<15	<17
Unit mass	g/cm^3	Result	1640	1830	1850	1910
		Limit	>1250	>1250	>1250	>1250
Fines Content	%	Result	0.3	0.1	0.4	0.3
		Limit	<1	<1	<1	<1
Friable Materials* (FM)	%	Result	0.8	0.1	0.5	0.1
		Limit	<0.5	<0.5	<0.5	<0.5
L.A.A.	%	Result	17.6	22.6	18.1	10.7
		Limit	<30	<35	<35	<30
Soundness (Na_2So_4)	%	Result	0	0.08	0.19	0.4
		Limit	<10	<10	<10	<10
UCS	MPa	Result	83	125	106	175
		Limit	>100	>100	>100	>100
Micro-Deval*	%	Result	26.9	9.5	14.5	9.7
		Limit**	<14	<14	<14	<14

*Optional Tests – NBR 5564.
**Limit specified in EN-13450, without reference value in NBR 5564.

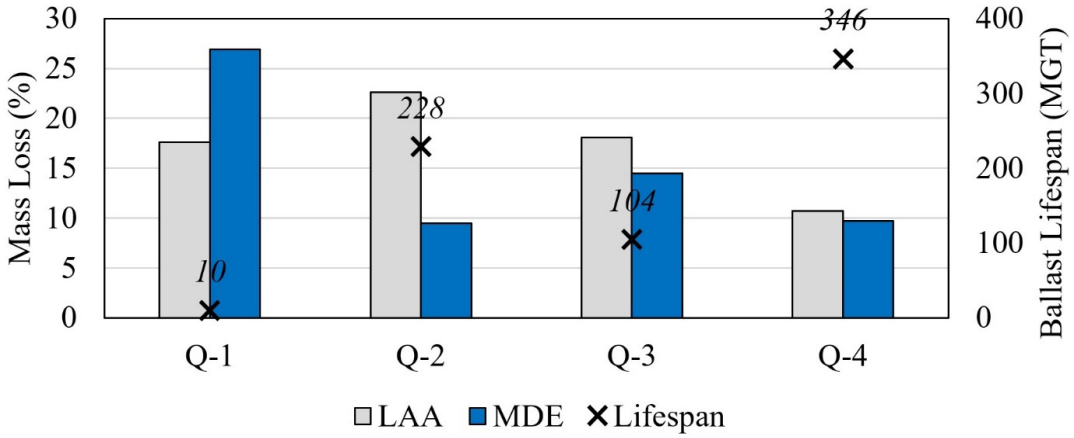

Figure 5. Ballast lifespan estimation using the CPR model. (LAA: Los Angeles Abrasion, MDE: Micro Deval).

3. TRACK DESIGN APPLICATION

3.1. Mechanical tests

The characterization tests provide information about the durability of the ballast material, but the results are not directly linked to the design of the ballast layer. For design purposes, it would be beneficial to conduct cyclic loading tests, such as those assessing R_M and permanent deformation under various stress states), to more accurately predict the durability of the ballast material.

Real-scale ballast triaxial tests require a minimum ratio between the diameter of the particles and the specimen of 6 times (Merheb et al., 2014; Skoglund, 2002), also recommended by the in D5311 (ASTM, 2012) cyclic triaxial procedure, resulting in a specimen diameter of about 381 mm (6 times 63.5 mm). Normally, literature parameters are adopted for the ballast layer. In the present research, the University of São Paulo equipment was used, with specimen size of 400x800 mm (diameter x height). First, the material from each quarry was divided into four portions, each with equal mass and PSDs. The material was then submerged for 24 hours to allow water to enter the apparent pores of the particles. The portions were placed inside the cylindrical mold, and each was vibrated using a vibrator attached to a circular steel plate. After all the material was placed inside the mold, the compacted bulk density was measured, the top face was regularized with plaster, and a top-cap and O-ring were inserted. The sample was moved to the press, and a suction of 45 kPa was applied to generate vacuum and remove the walls of the mold. The sequence is presented in Figure 6.

The first loading stage consisted in applying 1,000 cycles of $\sigma_3 = \sigma_d = 75$ kPa. Then the R_M test was performed with 200 cycles in each stress state (Table 2), these configurations were chosen in a way to reduce the permanent deformations during the loading step. After, the permanent deformation test was performed in three stress states (Table 2), with 50,000 cycles each. The number of cycles was sufficient for the stabilization of the permanent settlement trend and above the adopted for σ_1 / σ_3 up to 4 in similar studies (Diógenes, Castelo Branco and Motta, 2020; Merheb et al., 2014). All the combinations of σ_3 and σ_1 were selected based on simulations that were performed before the laboratory tests, with literature materials (Merheb et al., 2014; Nålsund, 2014). They also converged with the values observed in the simulations performed with the characterized materials, which showed ballast peak confining stress of 70 kPa, while the peak deviatoric stress was 210 kPa.

Figure 6. (a) Sample Quartering; (b) Submersion; (c) Mold filling; (d) Sample densification; (e) Top-cap placement; (f) Vacuum application.

In the case of subgrade material, since the variations in its properties are not the aim of the present study, only one material obtained along the project was considered in the simulations. The subgrade R_M test was performed according to DNIT ME/134 (similar to AASHTO T-307) and permanent deformation following DNIT IE/179 (similar to the Australian AGPT-T053-07).

Table 2: Triaxial tests configuration.

Test	Number of Cycles	σ3 (kPa)	σ1 (kPa)	σ1/σ3
Resilient Modulus	200 for each stress state	45	90	2
		45	135	3
		60	120	2
		60	180	3
		75	150	2
		75	225	3
Permanent deformation	50,000	60	120	2
	50,000	60	180	3
	50,000	60	240	4

3.2. Structural analysis

Aiming to understand the influence of different ballast materials on the railway track design, a finite elements model was developed using ABAQUS software. The simulation considered a track using 136RE rails, nylon rail pads, broad gauge, concrete sleepers, and applied directly onto the

final subgrade layer. The subballast was disregarded to reduce the number of variables. The track was modeled using transverse symmetry conditions, and infinite elements were utilized at the model boundaries to extend the subgrade (Khan and Dasaka, 2020; Li, Nimbalkar and Zhong, 2018; Shih, Thompson and Zervos, 2016). Using infinite elements has been shown to stabilize subgrade strains, preventing them from increasing indefinitely as the model dimensions increase.

HFT wagons filled with grains, with axle loads up to 32.5 t/axle and a maximum speed of 80 km/h, are included as inputs for the project. The most critical loading case occurs in the region between two adjacent bogies from different wagons. Therefore, the simulation focused on this isolated region, and the loads were increased by the AREMA impact factor to account for expected dynamic loading amplifications. The geometry of the HFT wagon and the model is depicted in Figure 7, illustrating the applied boundary conditions relevant to the analysis.

A mesh convergence analysis was conducted for each track component, first individually and then combined in the simulation. The analysis aimed to determine the optimum mesh size, ensuring that vertical displacements of the rail and subgrade stress varied by less than 2%. The results indicated convergence using the mesh elements detailed in Table 3, along with the assigned properties in the model. The rail, rail pads and sleepers were represented using hexahedral quadratic elements C3D20R, chosen for their suitability in capturing the structural behavior of these components. Meanwhile, tetrahedral C3D10 elements were selected for modeling the geotechnical aspects, considering their efficiency in representing soil mechanics. All the Poisson's ratio were obtained from literature (Rodrigues and Dimitrovová, 2021).

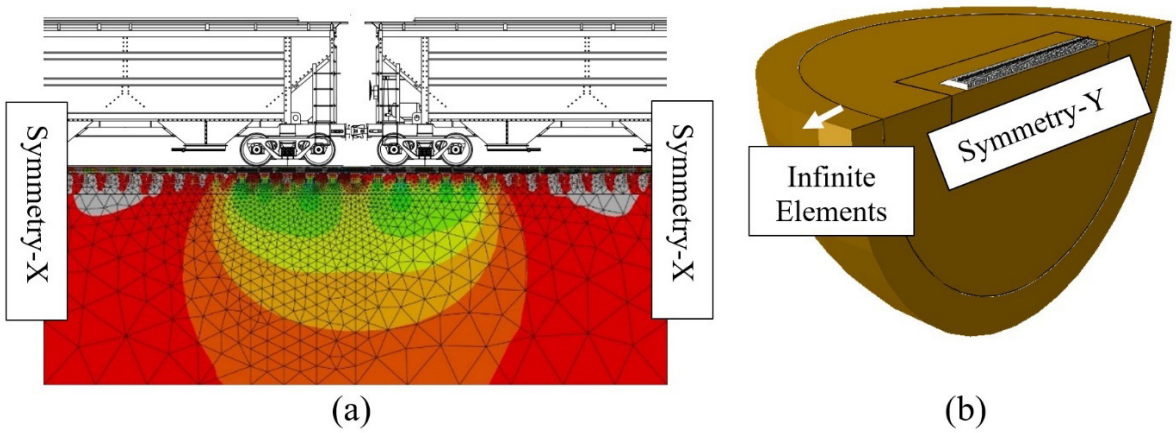

Figure 7. (a) Longitudinal section; (b) Whole model.

A User Material (UMAT) subroutine was implemented to iteratively calculate the stress state and R_M in each geotechnical element for every new strain increment (Kim, Tutumluer and Kwon, 2009; Kuo and Huang, 2006). The principal stresses in each model element are used as input to calculate R_M values, using the combined model and the regression coefficients defined for each geotechnical layer. The code covers not only the resilient behavior of the geotechnical materials, but also the granular characteristic of the ballast, limiting the occurrence of tension regions inside the layer. In contrast to elastic analysis, plastic strains were computed in a post-processing step. This involved extracting the stress state of each element and calculating the permanent deformation part, allowing for a comprehensive understanding of the material's behavior beyond elastic limits. The residual stresses related to ground compaction were disregarded from the analysis, considering that the subgrade is a naturally formed material, without influence of compaction equipment's.

Table 3: Track components, mesh size and mechanical parameters used in the simulation.

Component	Min-Max Element Size (mm)	Elastic Parameters
Rail	5-100	$\upsilon = 0.25; E = 210,000\,MPa$
Rail Pad	5-50	$\upsilon = 0.40; E = 1,000\,MPa$
Sleeper	20-50	$\upsilon = 0.2; E = 30,000\,MPa$
Ballast (Q-1)	75-200	$\upsilon = 0.35$; $R_M = 644.4\sigma_3^{0.31}\sigma_d^{0.09}$
Ballast (Q-2)	75-200	$\upsilon = 0.35$; $R_M = 310.5\sigma_3^{-0.06}\sigma_d^{0.39}$
Ballast (Q-3)	75-200	$\upsilon = 0.35$; $R_M = 371.3\sigma_3^{0.06}\sigma_d^{0.31}$
Ballast (Q-4)	75-200	$\upsilon = 0.35$; $R_M = 756.9\sigma_3^{0.37}\sigma_d^{0.18}$
Subgrade	100-2000	$\upsilon = 0.30; R_M = 177.0\sigma_3^{0.04}\sigma_d^{0.164}$

υ is the Poisson's ratio, E the elastic modulus, R_M the resilient modulus and σ_3 and σ_d the confining and deviatoric stress, respectively.

Five scenarios were simulated for each quarry material, varying ballast thickness (e) from 10 to 50 cm. Subsequently, results of subgrade stresses and rail vertical displacements were extracted and tabulated in Table 4 for analysis and comparison.

In the simulations, the peaks of ballast R_M were 294, 115, 140 and 242 MPa, for quarries from Q-1 to Q-4, respectively. The results indicated that vertical displacements remained practically unchanged, especially due to the similarity between ballast and subgrade R_M. The obtained vertical stresses varied from 166 to 154 kPa in the case of 100 mm thickness ballast and from 95 to 89 kPa for 500 mm ballast.

A non-linear relation between ballast thickness and subgrade stresses was determined, for both vertical and confining stresses, showing that reducing the ballast thickness increases the stresses at the top of the subgrade (Doyle, 1980). The comparison of subgrade acting stresses and the subgrade allowable stresses provides information for optimizing the ballast thickness in terms of ballast volume and consequently the construction costs. But this optimization is only possible with a drawback in terms of subgrade stresses and a detailed analysis should be performed for its evaluation, to assure that these stresses would not comprise the railway's formation integrity with the seasonal variations in the soil saturation degree.

The subgrade primarily comprises fine and medium sand (57%), with less than 40% material passing the #200 sieve. This material exhibits lateritic behavior (classified as LA'), characterized by a high initial void ratio of 1.1. The undisturbed dry density measured was around 1.2 kg/m^3, increasing to 1.7 g/cm3 after compaction. The direct shear test revealed a friction angle of 29º and a cohesion of 17.7 kPa. However, for the calculation of SBC the cohesion was disregarded due to the observed natural cementing characteristic of this type of soil. Using only the second term of Broms method equation, the subgrade ultimate stress was determined to be 310 kPa. Applying a safety factor of 2.5 (Sattler et al., 1989), the SBC value of 124 kPa was obtained for practical application.

The resulted values are plotted along with the subgrade stresses for all the quarries in Figure 8. Based on the calculated SBC, it is recommended to design the ballast with a thickness between 24 and 28 cm. The thinnest recommended thickness is achieved using Q-1 material, while the thickest

is with Q-4 material. Furthermore, the analysis indicates that reducing the ballast thickness from 50 cm to 10 cm almost doubles the subgrade stresses. This underscores the importance of careful consideration in ballast design to mitigate excessive stress on the subgrade.

Table 4: Resulted subgrade stresses and rail vertical displacements.

Quarry	e (mm)	σ1 (kPa)	σ3 (kPa)	σ1/σ3	δv (mm)
Q-1	100	154.19	28.37	5.43	3.18
	200	131.86	26.06	5.06	3.16
	300	112.93	24.65	4.58	3.14
	400	94.77	20.84	4.55	3.12
	500	89.15	19.41	4.59	3.10
Q-2	100	162.82	31.31	5.20	3.19
	200	134.18	26.01	5.16	3.16
	300	116.96	22.58	5.18	3.14
	400	101.57	20.20	5.03	3.12
	500	94.58	18.75	5.04	3.10
Q-3	100	162.16	31.05	5.22	3.20
	200	134.07	26.70	5.02	3.18
	300	117.12	23.23	5.04	3.17
	400	100.38	20.89	4.80	3.15
	500	93.57	19.68	4.76	3.14
Q-4	100	166.25	33.44	4.97	3.23
	200	139.60	28.90	4.83	3.22
	300	120.11	25.26	4.75	3.23
	400	100.34	22.64	4.43	3.22
	500	94.10	21.84	4.31	3.22

e is the ballast depth, δ_v is the elastic deformation, σ_3 the confining stress and σ_1 the highest principal stress.

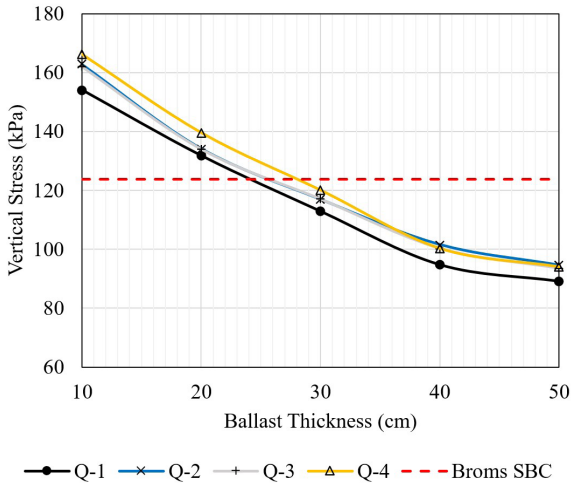

Figure 8. Relation between ballast thickness and subgrade maximum vertical stress.

3.3. Geometry degradation

To calculate the permanent deformations of the ballast, the average deviator and confining stresses at each calculation point was determined. Then, the relationship between these two

stresses were calculated, and Equation 3 was employed to calculate the permanent deformation, as there was little variation in σ1 and σ3 during the tests. For values of σ1/σ3 between two and three or between three and four, a linear estimation using both curves were employed. For the calculation of subgrade permanent deformation, the same procedure was used to extract the FEM model data, but the results were directed applied to the Guimarães Equation 4. The number of loading cycles used to estimate permanent deformation was 4.7×10^7, which represents 30 years of track operation and more than 1,500 MGT, considering that during this period only routine maintenance for track geometry would be performed. The results for each quarry material are presented in Figure 9. Similar to the AREMA geometry limits, in Brazil the NBR 16387 (ABNT, 2020) prescribes the limits for vertical alignment in tangent track, which for broad gauge and train speed up to 80 km/h is 36 mm. This value was adopted as limit for track permanent deformation, as a reference for the comparison between the simulation results.

It has been observed that the subgrade significantly influences the total permanent settlement of the track. In most cases, reducing ballast thickness results in increased permanent settlement. However, the behavior of Q-4 material deviated from this trend, showing greater ballast settlement but a reduction in overall track settlement when ballast thickness was reduced. This behavior may be linked to the high proportion of non-cubic particles in the Q-4 material, which can lead to an unstable ballast layer. Ultimately, the Q-4 material exhibited the poorest performance in terms of resistance to ballast track settlement.

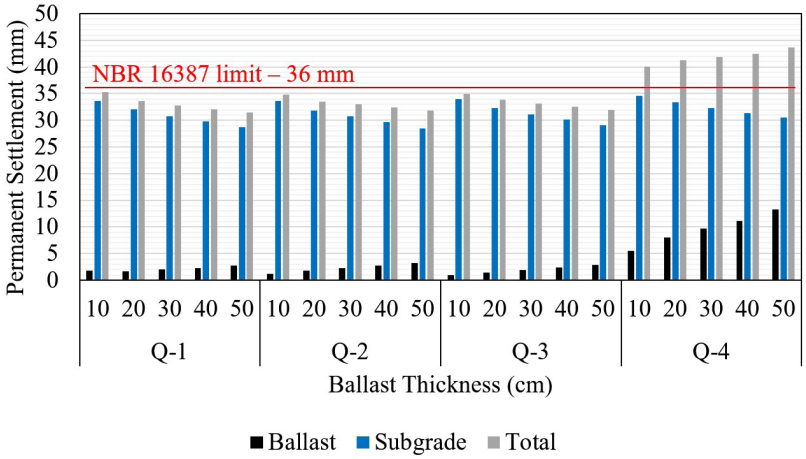

Figure 9. Permanent deformation for each simulated scenario.

4. MATERIAL COMPARISON

The application of four different ballast materials in a new railway project in Brazil was evaluated. Ballast particles were analyzed considering the aspects of physical characteristics, strength to mechanical and chemical degradation. Furthermore, a numerical approach was used to investigate the influence of ballast layer material and thickness on subgrade stresses, later analyzing its relationship with subgrade failure and track permanent deformation. Regarding the evaluated aspects, a rank from 1 (best) to 4 (worst) is attributed to the quarry materials in Table 5 and material Q-2 is elected as the most suitable material for this construction, due to its overall performance. This overall performance was assessed not only based on the mechanical properties of the layer but also in terms of the physical characteristics of the particles, which are closely linked to the short- and long-term degradation of the ballast.

Table 5: Quarry materials rank.

Evaluated Aspects	Q-1	Q-2	Q-3	Q-4
Geological Classification	Sandstone	Granite	Granite	Basalt
Particles Physical Characteristics	4	1/2	3	1/2
Particles Strength to Mechanical and Chemical Degradation	4	1/2	3	1/2
Estimated Lifespan (CPR formulation)	4	2	3	1
Ballast Thickness Necessity	1	2/3	2/3	4
Track Permanent Deformation	1/2/3	1/2/3	1/2/3	4

5. CONCLUSIONS

The following conclusions could be drawn from the results obtained in the paper:

- Four materials with different geological characteristics and particle size distributions (PSDs) were tested, with peak R_M values between 294 and 115 MPa, but these materials exhibited similar stress attenuation capacities;
- The relationship between ballast thickness and subgrade stresses is non-linear, with an increase from 10 to 20 cm resulting in a 19% attenuation of subgrade vertical stress, while an increase from 40 to 50 cm attenuates only 7%;
- Material Q-4 demonstrates favorable mechanical characterization results, but it surpasses the threshold for the non-cubic percentage. This could explain the high permanent deformations observed in the cyclic triaxial tests with this material;
- Evaluating ballast wear resistance, especially in wet conditions, is crucial. Tests such as Micro-Deval or Mill Abrasion are valuable for assessing wear resistance under such conditions, as materials with low LAA values may still exhibit poor wet abrasion results;
- Although the design using Q-1 material resulted in good stress attenuation and permanent deformation bellow the standard limits, the lifespan calculated using M_{DE} value indicated that a ballast maintenance would be needed with only 10 MGT. Therefore, the material was disqualified;
- Material properties such as absorption, porosity, and apparent density may hold varying levels of importance across different projects. In regions unaffected by freeze-thaw cycles, materials with good wet abrasion resistance may allow the use of high porosity materials. Further studies are warranted to explore these aspects comprehensively.

AUTHORS' CONTRIBUTIONS

André Fardin Rosa: Formal analysis, Data curation, Writing – original draft, Writing – review & editing, Methodology, Software, Validation; Stefanie de Carla Dias: Conceptualization, Visualization; Wescley Silva Brito: Funding acquisition; Robson Correia Costa: Investigation; Edson de Moura: Resources; Liedi Légi Bariani Bernucci: Project administration; Rosângela dos Santos Motta: Supervision.

CONFLICTS OF INTEREST STATEMENT

Nothing to declare.

USE OF ARTIFICIAL INTELLIGENCE-ASSISTED TECHNOLOGY

The authors declare that no artificial intelligence tools were used in the research reported here or in the preparation of this article.

ACKNOWLEDGEMENTS

The authors gratefully acknowledge Rumo S.A. and the University of São Paulo for supporting the study.

REFERENCES

ABNT (2020). NBR 16387, Via férrea - Classificação de vias. Rio de Janeiro: ABNT.

ABNT (2021). NBR 5564, Via férrea - Lastro ferroviário. Rio de Janeiro: ABNT.

AREMA. (2020). Manual for Railway Engineering. Lanham: AREMA.

ASTM (2012). D5311, Standard Test Method for load controlled cyclic triaxial strength of soil. West Conshohocken: ASTM.

Diógenes, D.F.; V.T.F. Castelo Branco and L.M.G. Motta (2020) Avaliação da relação entre comportamentos mecânico e hidráulico para lastro ferroviário. *Transportes*, v. *28*, n. 3, p. 61-74. DOI: 10.14295/transportes.v28i3.1829.

Doyle, N.F. (1980). *Railway Track Design: A Review of Current Practice. Canberra: Australian Government Publishing Service.*

Guimarães, A.C.R. (2009). *Um Método Mecanístico-Empírico para a Previsão da Deformação Permanente em Solos Tropicais Constituintes de Pavimentos.* Tese (doutorado). Universidade Federal do Rio de Janeiro, Rio de Janeiro. Available at: <http://www.coc.ufrj.br/pt/teses-de-doutorado/153-2009/1199-antonio-carlos-rodrigues-guimaraes> (accessed 07/07/2024)

Khan, M.R. and S.M. Dasaka (2020) EPS geofoam as a wave barrier for attenuating high-speed train-induced ground vibrations: a single-wheel analysis. *International Journal of Geosynthetics and Ground Engineering, v. 6*, n. 4, p. 43. DOI: 10.1007/s40891-020-00230-1.

Kim, M.; E. Tutumluer and J. Kwon (2009) Nonlinear pavement foundation modeling for three-dimensional finite-element analysis of flexible pavements. *International Journal of Geomechanics, v. 9*, n. 5, p. 195-208. DOI: 10.1061/(ASCE)1532-3641(2009)9:5(195).

Kuo, C. and C. Huang (2006) Three-dimensional pavement analysis with nonlinear subgrade materials. *Journal of Materials in Civil Engineering, v. 18*, n. 4, p. 537-44. DOI: 10.1061/(ASCE)0899-1561(2006)18:4(537).

Lackenby, J.; B. Indraratna; G. McDowell et al. (2007) Effect of confining pressure on ballast degradation and deformation under cyclic triaxial loading. *Geotechnique*, v. *57*, n. 6, p. 527-36. DOI: 10.1680/geot.2007.57.6.527.

Li, D.; J. Hyslip; T. Sussmann et al. (2016). *Railway Geotechnics. Boca Raton: CRC Press.*

Li, L.; S. Nimbalkar *and* R. Zhong *(*2018*) Finite element model of ballasted railway with infinite boundaries considering effects of moving train loads and Rayleigh waves. Soil Dynamics and Earthquake Engineering, v. 114*, p. 147-53. DOI: 10.1016/j.soildyn.2018.06.033.

Lima, C. and L. Motta (2016) Study of permanent deformation and granulometric distribution of graded crushed stone pavement material. *Procedia Engineering, v. 143*, p. 854-61. DOI: 10.1016/j.proeng.2016.06.141.

Merheb, A.H.M.; R. Motta; L. Bernucci et al. (2014) Equipamento triaxial cíclico de grande escala para análise mecânica de lastro ferroviário. *Transportes, v. 22*, n. 3, p. 53. DOI: 10.14295/transportes.v22i3.804.

Monismith, C.L. (1976) Rutting prediction in asphalt concrete pavements. *Transportation Research Record: Journal of the Transportation Research Board, p.* 616.

Nålsund, R. *(*2014*). Railway Ballast Characteristics, Selection Criteria and Performance. Thesis.* University of Science and Technology, Trondheim. Available at: <http://hdl.handle.net/11250/233318> (accessed 07/07/2024)

Ramūnas, V.; A. Vaitkus; A. Laurinavičius et al. (2017) Raudteeballasti tööea prognoos lähtudes selle mehhaanilistest omadustest. *The Baltic Journal of Road and Bridge Engineering, v. 12*, p. 203-9. DOI: 10.3846/bjrbe.2017.25.

Rodrigues, A.F.S. and Z. Dimitrovová (2021) Applicability of a three-layer model for the dynamic analysis of ballasted railway tracks. *Vibration*, v. *4*, n. 1, p. 151-74. DOI: 10.3390/vibration4010013.

Rosa, A.F. (2019). *Efeito da Granulometria e da Litologia no Comportamento de Lastros Ferroviários em Laboratório e por Análise Computacional.* Dissertação. Universidade Federal do Rio de Janeiro, Rio de Janeiro. Available at: <https://pantheon.ufrj.br/handle/11422/13988> (accessed 07/07/2024)

Santos, R.S.; R.P. Ribeiro; A.B. Paraguassú et al. (2021) Railroad ballast of granites and basic rock in tropical regions: relationships between petrography, physical-mechanical properties and alterability. *Transportes, v. 29*, n. 2. DOI: 10.14295/transportes.v29i2.2369.

Sattler, P.; D.G. Fredlund; M.J. Klassen et al. (1989) Bearing capacity approach to railway design using subgrade matric suction. *Transportation Research Record: Journal of the Transportation Research Board, p.* 27-33.

Selig, E.T. *and* D.L. Boucher *(*1990*) Abrasion tests for railroad ballast. Geotechnical Testing Journal, v. 13*, n. 4, p. 301-11. DOI: 10.1520/GTJ10173J.

Shih, J.Y.; D.J. Thompson and A. Zervos (2016) The effect of boundary conditions, model size and damping models in the finite element modelling of a moving load on a track/ground system. *Soil Dynamics and Earthquake Engineering, v. 89*, p. 12-27. DOI: 10.1016/j.soildyn.2016.07.004.

Skoglund, K.A. (2002). *A Study of Some Factor in Mechanistic Railway Track Design. Thesis.* Norwegian University of Science and Technology, *Trondheim.* Available at: <https://ntnuopen.ntnu.no/ntnu-xmlui/handle/11250/231131> (accessed 07/07/2024)

Sun, Q.D.; B. Indraratna and S. Nimbalkar (2016) Deformation and degradation mechanisms of railway ballast under high frequency cyclic loading. *Journal of Geotechnical and Geoenvironmental Engineering, v. 142*, n. 1, p. 04015056. DOI: 10.1061/(ASCE)GT.1943-5606.0001375.

Trotta, R.P. (2020). *Quantificação da Degradação Mecânica e Avaliação da Heterogeneidade de Agregados por Processamento de Imagem (PDI).* Dissertação. Universidade do Rio de Janeiro, Rio de Janeiro.

Uzan, J. (1985) Dynamic characterization of granular materials. *Transportation Research Record: Journal of the Transportation Research Board, p.* 52-9*.*

Watters, B.R.*;* M.J. Klassen *and* A.W. Clifton *(*1987*) Evaluation of ballast materials using petrographic criteria. Transportation Research Record: Journal of the Transportation Research Board, p.* 45-58. Available at: <https://trid.trb.org/view/282807> (accessed 07/07/2024).

Werkmeister, S.; A. Dawson and F. Wellner (2001) Permanent deformation behavior of granular materials and the shakedown concept. *Transportation Research Record: Journal of the Transportation Research Board, v. 1757*, n. 1, p. 75-81. DOI: 10.3141/1757-09.